SU(3) Kondo effect in spinless triple quantum dots

Rosa López,[1,2] Tomaž Rejec,[3,4] Jan Martinek,[5] and Rok Žitko[3,4]

[1]*Institut de Física Interdisciplinària i de Sistemes Complexos IFISC (CSIC-UIB), E-07122 Palma de Mallorca, Spain*

[2]*Departament de Física, Universitat de les Illes Balears, E-07122 Palma de Mallorca, Spain*

[3]*Faculty of Mathematics and Physics, University of Ljubljana, Jadranska 19, SI-1000 Ljubljana, Slovenia*

[4]*Jožef Stefan Institute, Jamova 39, SI-1000 Ljubljana, Slovenia*

[5]*Institute of Molecular Physics, Polish Academy of Sciences, Smoluchowskiego 17, 60-179 Poznań, Poland*

(Received 29 August 2012; revised manuscript received 6 December 2012; published 28 January 2013)

We discuss a device—a purely capacitively coupled interacting triple quantum dot system in an external magnetic field—for the observation of the SU(3) Kondo effect, identified by the conductance being pinned to a characteristic value of 3/4 of the unitary limit. The Kondo effect occurs in two plateaus where the dot occupancy is pinned to an integer value, either 1 or 2. We discuss the thermodynamic and spectral properties of the corresponding triple-impurity model and establish how the presence of SU(3) Kondo screening can be identified in the temperature dependence of the conductance through one of the dots. We report results about the robustness of the SU(3) Kondo effect against various perturbations present in real experimental setups, namely unequal reservoir-dot tunneling couplings, gating effects, and nonvanishing interdot tunneling rates. Finally, we describe possible mechanisms to restore the SU(3) Kondo physics by properly tuning the on-site dot potentials. We briefly comment on the spinful case (i.e., the same system in the absence of the magnetic field), which has very different behavior and shows Kondo plateaus in conductance for all integer values of the occupancy, including at the particle-hole symmetric point.

DOI: 10.1103/PhysRevB.87.035135 PACS number(s): 72.10.Fk, 72.15.Qm

I. INTRODUCTION

In metals, magnetic impurities are responsible for the anomalous behavior of the resistivity at low temperatures.[1] Magnetic interactions result from high-order correlated tunneling of electrons that are hopping *in* and *out* of impurities. In this fashion, the impurity spin is screened through the formation of the Kondo spin-singlet state. In semiconductor quantum dots, the Kondo effect can also take place, as theoretically predicted[2–4] and experimentally observed.[5–7] Whereas the resistivity of a magnetically doped metal increases when the temperature is lowered below the Kondo temperature, T_K, in quantum dots (QDs) the linear conductance increases and eventually reaches its maximum value $G = 2e^2/h$ at zero temperature.[7] This is due to the enhancement of the scattering rate which results in the opening of a channel for electrons that are perfectly transmitted through the QD. The main advantage of exploring the Kondo effect in manufactured nanostructures such as QDs[5,6,8,9] is their high tunability. Using gate electrodes, it is possible to vary in a controllable manner the number of trapped electrons and the strength of the tunnel coupling between the reservoirs and the localized dot states. Furthermore, as an additional advantage, the QDs constitute perfect laboratories to test many-body effects under nonequilibrium conditions.[10–14] The influence of external fields such as finite bias voltages[12,13] or time-varying ac fields[11] allows the observation of the Kondo effect out of equilibrium.

Magnetic fields dramatically affect the Kondo state. The level degeneracy, required for the occurrence of the usual spin-1/2 Kondo effect, is lifted in the presence of the field. There are, however, some exceptions where a magnetic field facilitates the development of a Kondo state, for example in vertical QDs with an even number of electrons. Here, the integer-spin Kondo effect occurs when the singlet and triplet states become degenerate because of the presence of the magnetic field.[15–20] Therefore, in general, magnetic fields either remove the Kondo effect or facilitate its observation through the level degeneracy requirement.

The recent progress in fabricating highly tunable TQDs[21–25] aims to provide a platform for testing a variety of predicted novel quantum information processing functionalities and many-body effects.[26,27] The fabrication of more complex nanostructures has opened new possibilities for the study of the unconventional Kondo effect, for example in nanodevices based on carbon materials such as fullerenes, carbon nanotubes, and graphene.[28–37] Other systems, such as p-doped nanowires, have demonstrated the Kondo effect assisted by holes.[38] The search for highly symmetric Kondo singlets has been revived in carbon nanotubes and vertical double dot systems with the experimental demonstration of the SU(4) Kondo effect.[30,32,39–41] In carbon nanotubes, the valley isospin together with the spin degree of freedom manifests as a fourfold shell structure in the Coulomb blockade regime.[42,43] In the low-temperature regime, the fluctuations among the four quantum states lead to the observation of the SU(4) Kondo effect.[30,44,45] The SU(2) and SU(4) Kondo effects have been studied extensively. There are, however, very few works devoted to QD implementations of other possible symmetries for a Kondo singlet, in particular to the SU(3) Kondo effect. General properties of the SU(N) family of quantum impurity models have been studied using a variety of techniques,[46–52] mostly in the context of strongly correlated materials and magnetic dopants. In a recent work,[53] the SU(3) Kondo effect has been suggested to be observable in a triple quantum dot (TQD) in the quantum Hall regime. Here, we discuss a related setup—a spinless TQD with equal capacitative coupling V_i between all quantum dot pairs, as shown in the sketch in Fig. 1, as a suitable system for the observation of the SU(3) Kondo effect. An external magnetic field is used to fully polarize the

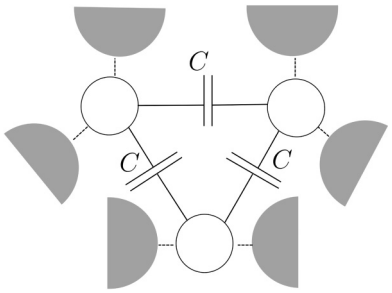

FIG. 1. Schematic representation of the capacitively coupled triple quantum dot system. Each quantum dot is attached to two electron reservoirs. We assume that a sufficiently large external magnetic field is applied to fully polarize the electrons, so that we may consider the system to be spinless. The only interaction between each pair of quantum dots is purely capacitive. Interdot charging energies (denoted by V) are assumed to be the same: they are characterized by the capacitance C, $V = e^2/2C$. Dashed lines indicate the electron transport through each dot.

electrons. The SU(3) Kondo physics takes place when there is a single electron or a single hole in the dots. This defines three possible *flavors* corresponding to the position of the electron (or hole) in one of the three dots or leads. In this work, we will refer to the flavor degree of freedom also as the *channel* or *orbital* degree of freedom; for our spinless model, these expressions are fully interchangeable. Each dot is connected to two contacts in such a way that the tunneling events conserve the flavor degree of freedom. Notice that in principle, this setup can be easily generalized to build an arbitrary SU(N) Kondo state,[53–57] although that would entail designing a device with equal capacitive coupling between all QD pairs. Importantly, the only interaction among the dots is capacitative and there is no particle exchange from one dot to the others, i.e., the interdot tunneling is not allowed since this would destroy the flavor conservation rule.

The goal of this work is to analyze the thermodynamic and transport properties of the SU(3) Kondo effect. A similar study (Ref. 58) has very recently been performed in parallel with our work and using an equivalent approach; where comparison can be made, our results agree with theirs. The main difference in the numerical technique (numerical renormalization group) in these two works is in the implementation of symmetries. The authors of Ref. 58 use the full SU(3) symmetry (or even higher symplectic symmetry) which greatly improves the calculation speed. In this work, however, we only use charge-conservation symmetry. While this implies much heavier computational requirements and somewhat less accurate results, it makes it possible to study the effect of various symmetry-breaking terms in the Hamiltonian which reduce the symmetry from full SU(3). An important part of our work is thus the study of the effect of various local perturbations on the SU(3) singlet Kondo state, such as asymmetrical lead-dot couplings, finite interdot tunneling rates, nonequal charging energies, etc. Generally, these perturbations destroy the SU(3) singlet Kondo state on low-energy and low-temperature scales. However, we propose a way to restore the Kondo resonance by properly gating the dot levels.

This paper is organized as follows. In Sec. II, we introduce the model Hamiltonian to describe the TQD setup and discuss the theoretical tools to solve it. Section III is devoted to the study of the emergence of the SU(3) Kondo regime as a function of various parameters, namely the dot level position (ϵ_i), the interdot Coulomb interaction (V_i), and the lead-dot tunneling couplings (Γ_i). The discussion is based on the thermodynamics and spectral properties. In Sec. IV, we list some signatures of the SU(3) Kondo state in the transport measurements. In Sec. V, we study the robustness of the SU(3) orbital Kondo singlet against diverse perturbations, namely asymmetric lead-dot tunneling couplings, different on-site energy values and possible leaking effects described by nonzero interdot tunneling rates. In Sec. VI, we briefly consider the generalization to the spinful "parent" problem and discuss the different kinds of Kondo effect expected in that case. Finally, our main conclusions are summarized in Sec. VII.

II. MODEL AND METHODS

We model the three QDs in a strong external magnetic field (see Fig. 1) using a Hamiltonian consisting of three copies of the (spinless) noninteracting resonant-level model (each describing one QD and the effective single channel of the electrons that the dot hybridizes with) and a coupling term which includes the interdot interactions and any possible interdot tunneling:

$$H = \sum_{i=1}^{3} H_i + H_{\text{int}}, \tag{1}$$

with

$$H_i = \sum_k \epsilon_k c_{k,i}^\dagger c_{k,i} + \epsilon_i d_i^\dagger d_i + v_i \sum_k (c_{k,i}^\dagger d_i + \text{H.c.}) \tag{2}$$

and

$$H_{\text{int}} = \sum_{\langle i,j \rangle} [V_{ij} n_i n_j + t_{ij} (d_i^\dagger d_j + \text{H.c.})]. \tag{3}$$

Here $c_{k,i}^\dagger$ is the creation operator for an electron with momentum k in channel i, while $d_i^\dagger$ is the creation operator for an electron in dot i; the occupancy operator is defined as $n_i = d_i^\dagger d_i$. Assuming flat conduction bands, the hybridization of each channel to the attached dot is characterized by a single number, $\Gamma_i = \pi \rho v_i^2$, where ρ is the density of states in the band which we take to be constant and of width $2D$ (flatband approximation). Hereafter, we consider all energies in units of the half-bandwidth, $D = 1$. V_{ij} is the charge repulsion between two dots, while t_{ij} is the hopping amplitude between two dots. For symmetrical configurations, we simplify the notation as $\epsilon \equiv \epsilon_i$, $t \equiv t_{ij}$, $V \equiv V_{ij}$. Notice that this model is similar to the Coqblin-Schrieffer SU(N) model.[61] The equivalence is established on low-temperature scales where the charge fluctuations are quenched. Assuming that the conduction bands are particle-hole (p-h) symmetric ($\epsilon_{-k} = -\epsilon_k$), the p-h transformation ($d_i^\dagger \to d_i, d_i \to d_i^\dagger, c_k^\dagger \to c_{-k}, c_k \to c_{-k}^\dagger$, etc.) leads to (up to irrelevant constants)

$$\tilde{H}_i = \sum_k \epsilon_k c_{k,i}^\dagger c_{k,i} + (-\epsilon_i) d_i^\dagger d_i + (-v_i) \sum_k (c_{k,i}^\dagger d_i + \text{H.c.}) \tag{4}$$

and

$$\tilde{H}_{\rm int} = \sum_{\langle i,j\rangle} [V_{ij}(1-n_i)(1-n_j) - t_{ij}(d_i^\dagger d_j + \text{H.c.})]. \quad (5)$$

Therefore,

$$\tilde{\epsilon}_i = -\epsilon - \sum_{\langle i,j\rangle} V_{ij}\,. \quad (6)$$

The model is p-h symmetric only for $t_{ij} = 0$, since finite interdot hopping breaks the bipartiteness. (The sign change of the hybridization v_i is of no physical consequence.) For a symmetric configuration, the model is p-h symmetric around the point $\epsilon = -V$. Therefore, the parameter $\delta = \epsilon + V$ is a measure of the departure from the p-h symmetry.

To investigate in a general framework the different regimes encountered for the the TQD system, we consider the operators of the SU(3) Lie algebra which describe the orbital (flavor) degree of freedom of the electrons. The thermodynamics analysis is performed by calculating the impurity orbital (flavor) susceptibility $\chi_{\rm imp}(T)$ and the impurity entropy $S_{\rm imp}(T)$. The SU(3) Kondo physics occurs when the QDs are tuned to single occupancy, $n = 1$, or double occupancy, $n = 2$, which is achieved *away from the particle-hole symmetric point*,[53,58] contrary to what happens in the more familiar SU(2) and SU(4) Kondo cases where at half-filling the Kondo effect is present. Consequently, the Kondo peak itself is not symmetric with respect to the chemical potential as visible in the spectral densities for each dot. These values of the occupancy have important consequences for the linear conductance. In accordance with the Friedel-Langreth sum rule, the linear conductance is $G = G_0 \sin^2\delta$, where the scattering phase shift δ is approximately given by $\delta = \pi n/N$; here $n = \langle \hat{n}\rangle$ is the total TQD occupation and $N = 3$, while G_0 is defined as $G_0 = e^2/h$ (note that we are considering a spinless system, thus the spin factor 2 is not present in G_0). Therefore, in the SU(3) Kondo regime with $n = 1$ and 2 one has[53]

$$G_{\rm Kondo} = \tfrac{3}{4} e^2/h. \quad (7)$$

This result must be compared to that at the p-h symmetric point where $\delta = \pi/2$, and thus[59,60]

$$G_{p\text{-}h} = e^2/h. \quad (8)$$

The standard (Gell-Mann) parametrization for the generators of the SU(3) Lie algebra is $K_a = \lambda_a/2$, with λ_a being Gell-Mann matrices. We thus define the SU(3) operators for the TQD system as

$$O_a^{(k)} = \sum_{ij} c_{k,i}^\dagger (K_a)_{ij} c_{k,j}, \quad O_a^{\rm imp} = \sum_{ij} d_i^\dagger (K_a)_{ij} d_j,$$
$$O_a^{\rm total} = O_a^{\rm imp} + \sum_k O_a^{(k)}, \quad (9)$$

where $a = 1,\ldots,8$, while i and j range over the three channels and k ranges over all conduction-band momenta. The Casimir operator of SU(3) is defined as

$$K_{\rm total}^2 = \sum_{a=1}^{8} \left(O_a^{\rm total}\right)^2. \quad (10)$$

In a fully SU(3) symmetric case, the traces $\text{Tr}(O_a^2)$ are all equivalent. In numerical calculations, it is thus sufficient to calculate the expectation value of a single O_a^2 operator; the most convenient choice is O_3^2. The expectation value of $\langle K_{\rm total}^2\rangle$ is then eight times this value.

The behavior of an impurity system can be analyzed by studying its thermodynamic properties. In the following section, we will consider the impurity orbital susceptibility $\chi_{\rm imp}(T)$ and the impurity entropy $S_{\rm imp}(T)$. These two quantities serve to establish the range of parameters for which the SU(3) spin Kondo physics is encountered. In the fundamental representation of SU(3), one has $\langle K^2\rangle = 4/3$. In the high-temperature regime where all eight dot states are equally probable, one has $\langle K^2\rangle = (6\times 4/3 + 2\times 0)/8 = 1$, since there are six singly occupied states (by either one electron or by one hole) and two states corresponding to a totally empty and a totally full system. The impurity SU(3) orbital susceptibility (more precisely, the impurity contribution to the total system orbital susceptibility) is defined as

$$\chi_{\rm imp}(T) = \beta\left[\langle K_{\rm total}^2\rangle(T) - \langle K_{\rm total}^2\rangle_0(T)\right], \quad (11)$$

where the bracket with subscript 0 denotes the result for the system without the dots (i.e., the Hamiltonian H consists only of the conduction bands). Here $\beta = 1/k_B T$ with k_B the Boltzmann constant. The value of $k_B T\chi(T)$, therefore, indicates the presence of a finite effective orbital *local moment* on the TQD and it can be used to classify the fixed points.[62,63]

The impurity entropy is a measure of the number of the effective degrees of freedom of the TQD at a given parameter configuration. It is defined through

$$S_{\rm imp}(T) = \frac{(E-F)}{T} - \frac{(E-F)_0}{T}, \quad (12)$$

where $E = \langle H\rangle = \text{Tr}[H\exp(-H/k_BT)]$ and $F = -k_BT\ln\text{Tr}[\exp(-H/k_BT)]$.

We also compute the dot spectral functions $A(\omega,T)$ and compute the differential conductance through each dot using the Meir-Wingreen formula as[64]

$$G(T) = G_0 \int_{-\infty}^{\infty} \left(-\frac{\partial f}{\partial \omega}\right) \pi\Gamma A(\omega,T) d\omega, \quad (13)$$

where $G_0 = e^2/h$ and $f = [1+\exp(\omega/k_BT)]^{-1}$ is the Fermi-Dirac distribution function; the chemical potential has been fixed at zero energy.

The calculations have been performed using the numerical renormalization-group method[62,63,65,66] as implemented in the "NRG Ljubljana" code. We have mostly used the discretization parameter $\Lambda = 8$ with the z-averaging over $N_z = 8$ values.[67–72] We have verified that such a large value of Λ still produces reliable results[68] by performing a convergence study as a function of Λ down to $\Lambda = 2$. In the NRG truncation, we have kept states with energy up to $10\omega_N$, where ω_N is the characteristic energy scale at the Nth NRG step, or at most 6000 states. For calculating the spectral functions, we have used the complete Fock space method.[73,74] Very recently, a study of the fully symmetric SU(3) model was performed with an implementation of the NRG which can explicitly use the SU(3) symmetry of the model to greatly simplify the calculations.[58] Here we only use the U(1) total-charge conservation symmetry, thus the calculations are significantly more time-consuming. However, our approach makes it possible to study the effects of the symmetry-breaking

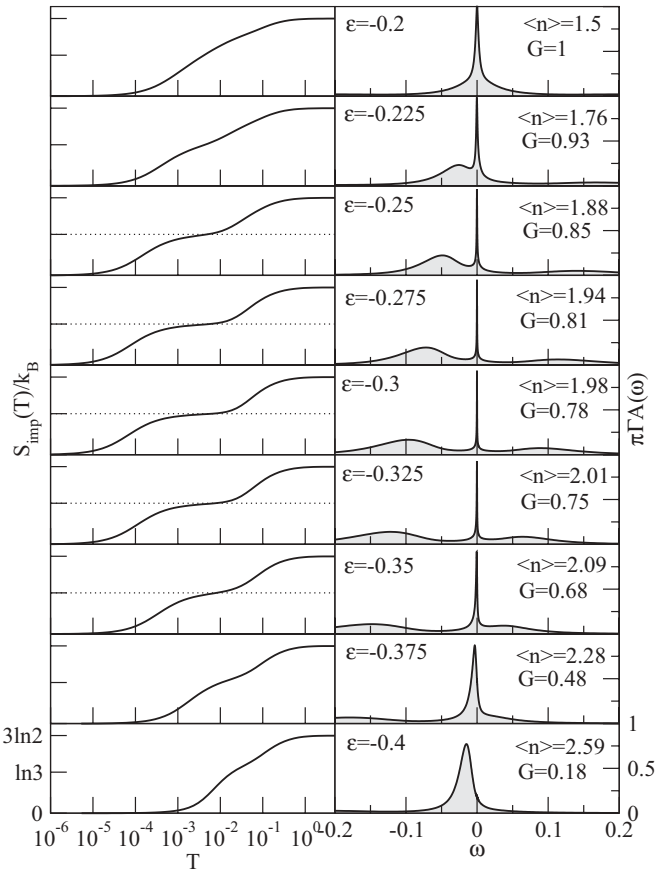

FIG. 2. Temperature dependence of the impurity entropy (left panels) and the $T = 0$ dot spectral function (right panels) for a range of the on-site energies ϵ. We consider a symmetric triple quantum dot system. The total occupancy of the triple quantum dot, $\langle n \rangle$, and the zero-temperature linear conductance through one dot, G, are also shown. The interdot tunneling is zero, $t = 0$. Other parameters are $\Gamma = 0.01$ and $V = 0.2$.

terms, which is important for physical realizations of this model.

III. NUMERICAL RESULTS: VALENCE FLUCTUATION AND THE SU(3) KONDO REGIMES

To identify the different regimes of the TQD system, we first consider the thermodynamic properties. In Fig. 2, we show the basic results for the fully SU(3) symmetric case in which all the dots and hybridizations are equivalent. The lead-dot couplings have a common value of $\Gamma = 0.01$, and there is no interchannel tunneling (i.e., $t \equiv 0$). Since the system is symmetric with respect to the point $\epsilon = -V$ for this choice of parameters, we consider only the value of the on-site energy ϵ below $-V$ (i.e., $\delta \leqslant 0$); other results can be obtained by an appropriate p-h transformation.

We observe that for a range of on-site energies $-0.35 \lesssim \epsilon \lesssim -0.25$, the occupancy reaches values close to 2 (see the $\langle n \rangle$ labels in the right panels of Fig. 2). In this gate-voltage range, the system evolves from the *free-orbital* fixed point (fp) with an impurity entropy of $3 \ln 2$ to a *local-moment* fp with triple degeneracy (indicated by a $\ln 3$ plateau in the impurity entropy) as the temperature decreases below the charge-fluctuation scale of V. The triple degeneracy is finally lifted at low temperatures and then we reach a *nondegenerate strong-coupling* fp corresponding to the SU(3) Kondo regime.

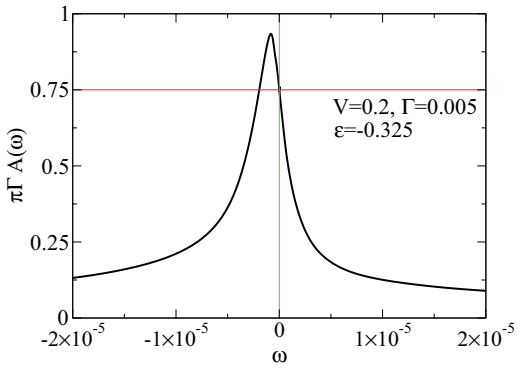

FIG. 3. (Color online) Spectral function in the SU(3) Kondo regime. The TQD is symmetric and $\langle n \rangle = 2$.

A very different behavior is found near the p-h symmetric point at $\epsilon = -V = -0.2$. Here the system evolves from the *free-orbital* to the *valence-fluctuation* fp with entropy $\ln 6$ [only visible as a weak bulge in the $S_{\rm imp}(T)$ curve in Fig. 2]. In this case, the valence-fluctuation regime corresponds to charge fluctuations from $n = 1$ to 2 charge states. The entropy is eventually reduced from $\ln 6$ to zero at some low temperature. In this case, the entropy is released as the system evolves to the *strong-coupling* fp without passing through the local-moment fp.

In the SU(3) Kondo regime, the dot spectral density, shown more clearly as a closeup in Fig. 3, displays a Kondo resonance with a maximum height away from the Fermi level. The shifted spectral density produces a zero-temperature linear conductance $G = 3/4(e^2/h)$, which is by itself a hallmark of the occurrence of the SU(3) Kondo physics, as predicted in Ref. 53 based on the Friedel sum rule arguments [see Eq. (1)]. This is in contrast with the SU(4) case in which the linear conductance coincides in value with the linear conductance for the SU(2) Kondo effect.

By reducing the dot-lead hybridization by half, i.e., for $\Gamma = 0.005$, as shown in Fig. 4, the SU(3) Kondo regime is even more clearly discernible and we can see that the occupancy is pinned to the value 2 for a much broader range of dot potential energies. Here, the conductance reaches the universal value of $G = 3/4(2e^2/h)$ for a wide range of ϵ due to a much more robust SU(3) Kondo state, although the Kondo temperature T_K is reduced.

To gain some intuition about the role of the Kondo correlations in the SU(3) orbital susceptibility, in Fig. 5 we compare the thermodynamic properties for the case of an uncoupled TQD system, where all three lead-dot hybridizations are $\Gamma = 0$, with the case in which the TQD is connected to leads and the SU(3) Kondo state builds up. In the high-temperature limit, in both cases the spin susceptibility is 1 and all eight TQD states are equally probable, thus there is $\ln 8 = 3 \ln 2$ impurity entropy. As the temperature decreases below V, so that the charge fluctuations are frozen out, the SU(3) susceptibility of $4/3$ is established, as expected for the fundamental triplet representation of SU(3). This is the *local-moment* fp. The decoupled system stays in this fixed point down to $T = 0$, while at finite Γ the local moment is screened in the SU(3)

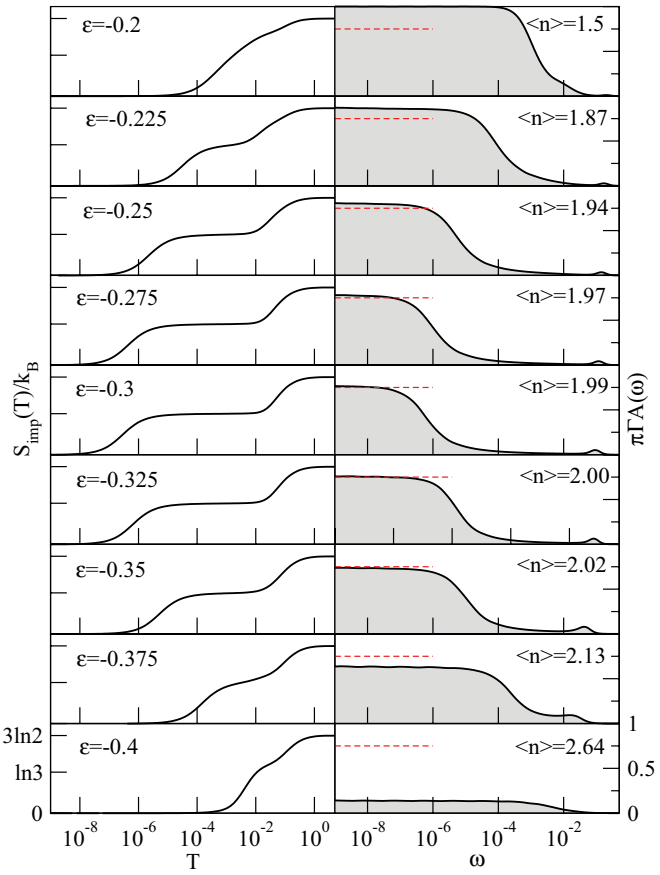

FIG. 4. (Color online) Temperature dependence of the impurity entropy (left panels) and the $T = 0$ dot spectral function (right panels) for a range of the on-site energies ϵ. Same parameters as in Fig. 2, but with smaller hybridization, $\Gamma = 0.005$. We plot the positive-frequency side of the spectral function on the *logarithmic* frequency scale. The dashed line corresponds to $G = (3/4)(e^2/h)$.

Kondo effect and the susceptibility vanishes, as expected. At this point the system is in the *nondegenerate strong-coupling* fp in which the ground state corresponds to a SU(3) Kondo singlet state. Notice that the transition from the *free-orbital* to the *local-moment* regime and then eventually to the *strong-coupling regime* is fully analogous to the behavior in the standard single-impurity Anderson model with the SU(2) symmetry.[62,63,65] We also emphasize that the low-temperature parts of the impurity susceptibility and impurity entropy are universal and that the scaling of the results for different parameters is observed if the temperature axis is rescaled by an appropriately defined Kondo temperature T_K (see below).

For completeness, we also analyze the *p-h* symmetric point, in which the only low-temperature scale is Γ itself and there is no Kondo-like screening. In this model, the *p-h* symmetric point corresponds to a valence-fluctuation regime where charge fluctuations occur. In Fig. 6, the temperature dependence of the entropy is shown for a symmetric TQD and various Γ values when $\epsilon = -V$. At high temperatures, the TQD is found in the free-orbital regime where the TQD entropy is $\ln 8$. Then, the system crosses over on the temperature scale of V to a valence-fluctuation fp with a sixfold-degenerate ground state in which the entropy reaches the value of $\ln 6$.

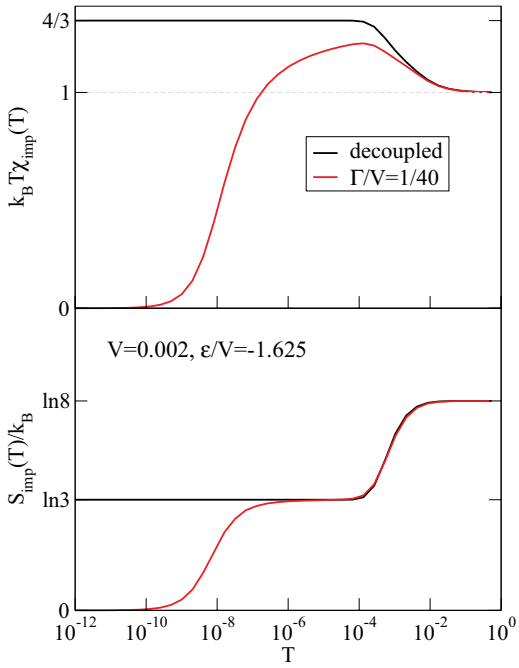

FIG. 5. (Color online) Thermodynamic properties in the SU(3) Kondo regime. The total occupancy is $\langle n \rangle = 2$. We compare the cases of a decoupled triple quantum dot system ($\Gamma = 0$) and the triple quantum dot connected to the leads ($\Gamma = 0.005$) in which the Kondo correlations are present.

In this case, there can be either a single electron or a single hole in the three dots for a total of six states with the same energy. Decreasing the temperature further, the system crosses over to the nondegenerate ground state with zero entropy at the temperature scale of Γ; see Fig. 6. There is no further dynamically generated low-energy scale in this case.

The zero-temperature fixed points for different ϵ form a line of fixed points which are related by the different strength of the residual potential scattering experienced by the quasiparticles. For an overview of the system behavior, in Fig. 7 we plot the

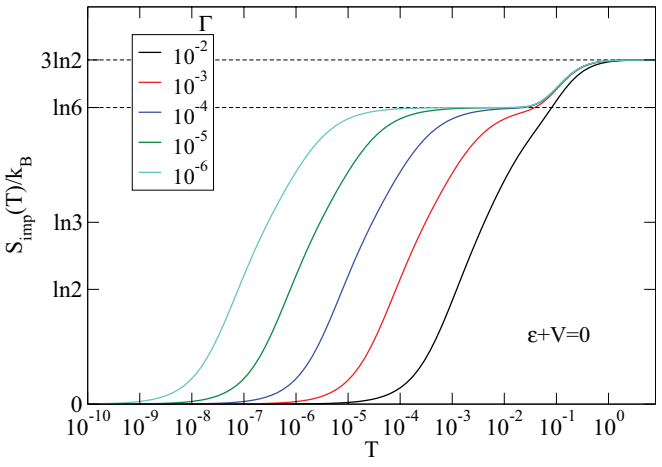

FIG. 6. (Color online) Temperature dependence of the entropy at the particle-hole symmetric point for a range of hybridization parameters Γ. We consider a symmetric triple quantum dot system with parameters $V = 0.2$ and $\epsilon = -V = -0.2$.

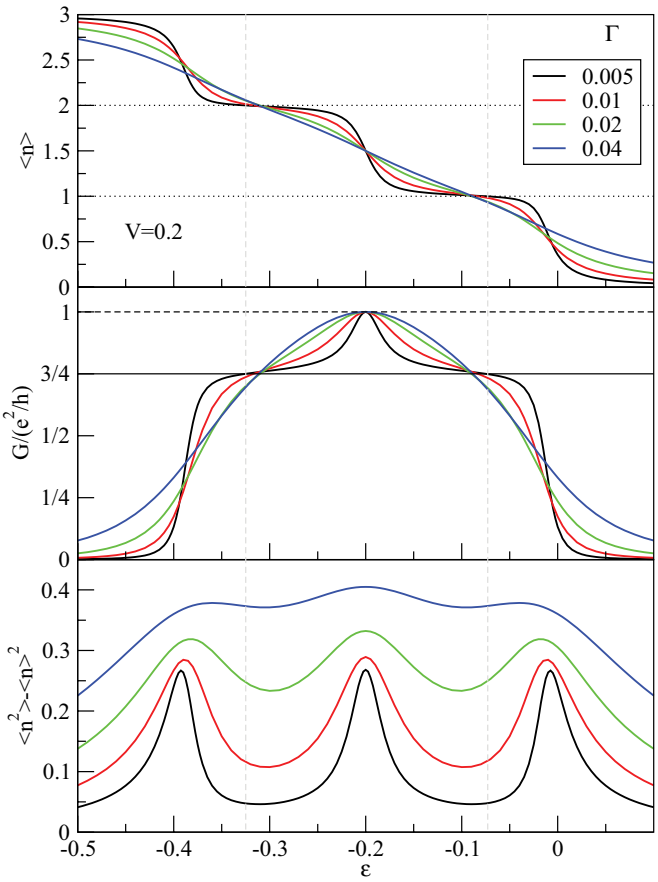

FIG. 7. (Color online) Occupancy n, differential conductance G, and charge fluctuations $\delta n^2 = \langle n^2 \rangle - \langle n \rangle^2$ as a function of the on-site energy for a range of hybridizations Γ.

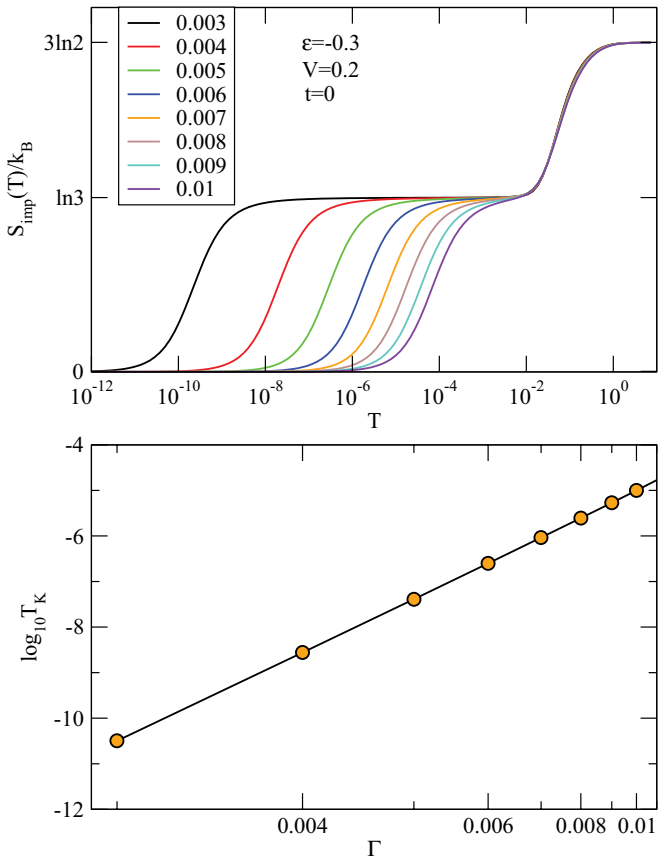

FIG. 8. (Color online) Top panel: Temperature dependence of the entropy for a symmetric triple quantum dot system for a range of hybridization parameters Γ. Other parameters are tuned so that the system is in the SU(3) Kondo regime, $V = 0.2$, $\epsilon = -0.3$. Bottom panel: Relation between the Kondo temperature T_K and the hybridization Γ. Here we use an arbitrary definition of the Kondo temperature, $S_{\rm imp}(T_K) = 0.1 k_B$.

zero-temperature total TQD occupancy, linear conductance, and charge fluctuations as a function of the on-site energy ϵ for several choices of the hybridization Γ. The emergence of the Kondo plateau for low enough Γ is clearly visible; it coincides with the regions of low charge fluctuations in the TQD. (These results are fully consistent with Fig. 1 in Ref. 58.)

IV. EVIDENCE OF SU(3) KONDO CORRELATIONS IN TRANSPORT MEASUREMENTS

In the preceding section, we demonstrated the occurrence of the SU(3) Kondo effect by considering the thermodynamic properties. Usually, one way to probe the existence of Kondo correlations in QD systems is to measure the exponential dependence of the Kondo energy scale ($k_B T_K$) with the inverse hybridization $1/\Gamma$ as

$$\ln T_K \propto -\frac{1}{\Gamma}. \tag{14}$$

In the NRG calculations, this dependence is demonstrated by using a T_K defined from the entropy curve as $S_{\rm imp}(T_K) = 0.1 k_B$; see the upper panel of Fig. 8. Plotting T_K for different Γ, we uncover the exponential dependence; see the lower panel of Fig. 8.

In view of this result, the occurrence of SU(3) Kondo correlations in a TQD experiment could be demonstrated by performing transport measurements, for instance by measuring the Kondo temperature T_K. Usually this is achieved by identifying the half-width at half-maximum (HWHM) of the nonlinear conductance peak through one of the dots with T_K. This measurement would, however, be rendered problematic in this system due to the asymmetric shape of the Kondo resonance. In dI/dV measurement with finite bias, the current is given approximately by

$$I(T,V) = \int [f_L(\omega) - f_R(\omega)] \pi \Gamma A(\omega, T) d\omega, \tag{15}$$

where we have neglected the voltage dependence of the spectral function, and we assume $f_L(\omega) = f(\omega - V/2)$ and $f_R = f(\omega + V/2)$. In the zero-temperature limit, we thus find approximately

$$\frac{dI}{dV} = G_0 \pi \Gamma \frac{A(V/2,0) + A(-V/2,0)}{2}. \tag{16}$$

Since the spectral function $A(\omega)$ is asymmetric, care is needed in extracting the width of the spectral function peak from the differential conductance measurements at finite bias voltage (even when the nonequilibrium effects are neglected). When

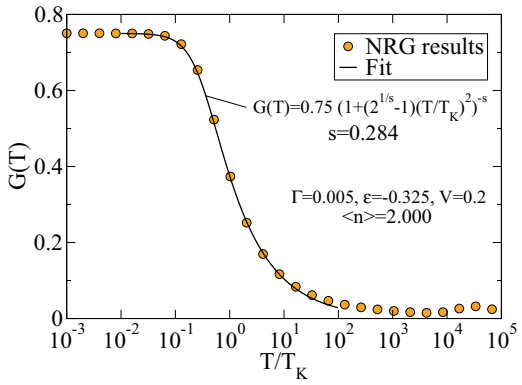

FIG. 9. (Color online) Temperature dependence of the linear conductance in the SU(3) Kondo regime of a symmetric triple quantum dot.

properly done, by measuring T_K and then varying Γ one should be able to get a relation that matches Eq. (14).

Another signature of the SU(3) Kondo physics could be detected through the temperature dependence of the linear conductance G. Close to zero temperature, G is 3/4 in units of the conductance quantum $G_0 = e^2/h$ (note the absence of factor 2 in this spinless case). At small but finite temperatures, we find that the low-temperature conductance fits, similarly to the SU(2) Kondo case, to the empirical formula of the general form[75]

$$G(T) = G_0[1 + (2^{1/s} - 1)(T/T_K)^2]^{-s}, \qquad (17)$$

with $s = 0.23$ for the SU(2) case and with $s = 0.28$ for the SU(3) Kondo case. The value of $s = 0.28$ has been extracted from the NRG results for $G(T)$. The fitting to $G(T)$ is performed for a symmetric TQD at $\epsilon = -0.2$ and $\Gamma = 0.005$; see Fig. 9. It is interesting to notice that a single fit formula, Eq. (17), applies over many orders of magnitude in temperature in a number of quantum impurity models that exhibit Kondo effects of very different kinds; see, for example, Refs. 75 and 76.

V. DEPARTURE FROM THE SU(3) STRONG-COUPLING FIXED POINT

In real experiments, it is extremely challenging to construct perfectly symmetric multidot systems. Therefore, in order to experimentally detect the SU(3) Kondo correlations, we need to know to what extent the SU(3) Kondo physics is robust against various local perturbations. These perturbation can arise from asymmetric lead-dot tunneling couplings, tunneling among the dots, and different on-site dot level potentials or distinct interdot Coulomb energies. In spite of the presence of unavoidable local perturbations in real setups that eventually destroy the SU(3) Kondo state, below we give a protocol to restore the Kondo correlations by properly adjusting the dot potentials.

A. Asymmetric lead-dot hybridizations

First, we analyze the effect of having asymmetric lead-dot coupling. If one of the hybridizations, say Γ_1, is made weaker, the SU(3) symmetry is broken. Even small changes of Γ_1 are sufficient; the effect is similar to the induced

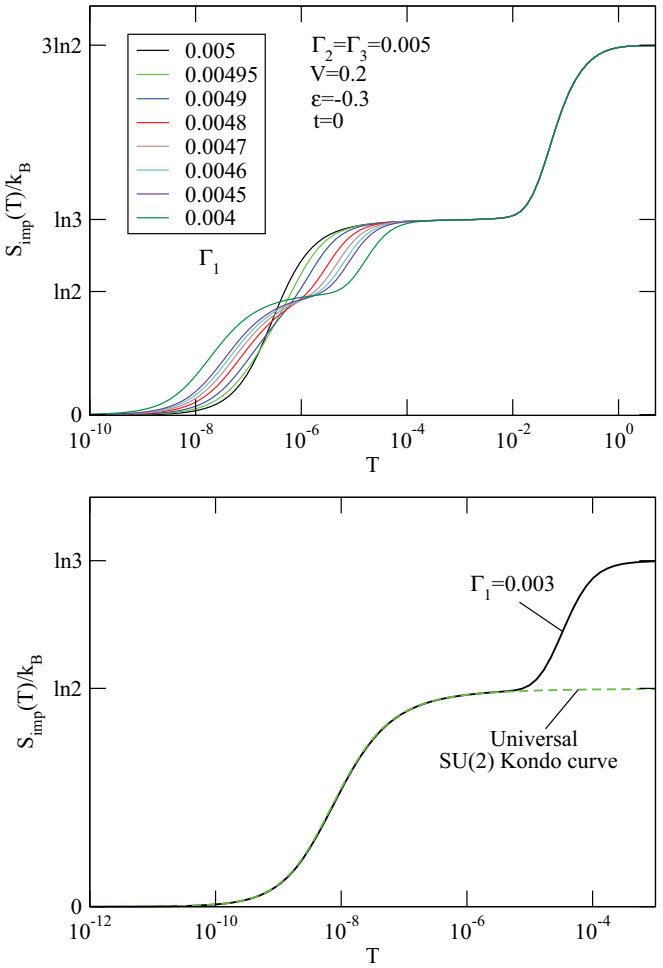

FIG. 10. (Color online) Top panel: Temperature dependence of the impurity entropy for a range of the hybridization parameter Γ_1, while $\Gamma_2 = \Gamma_3 = \Gamma$ is held fixed. Bottom panel: Impurity entropy for a strong symmetry breaking and a fit of the SU(2) Kondo screening crossover with the universal SU(2) entropy curve for the spinful single dot case.

magnetization by a ferromagnetic conduction band in the spinful single QD device. In the upper panel of Fig. 10, we show the impurity entropy evolution as the temperature is lowered for constant $\Gamma_2 = \Gamma_3 = \Gamma$ and Γ_1 ranging from $\Gamma_1 = \Gamma$ (symmetric configuration) to $\Gamma_1 = 0.9\Gamma$ (asymmetric lead-dot couplings). When the temperature is lowered, in the asymmetric lead-dot configuration the system flows from the SU(3) local-moment fp (with impurity entropy $\ln 3$) to a new SU(2) local-moment fp with twofold degeneracy (with impurity entropy $\ln 2$). The SU(2) local moment is then screened in the conventional SU(2) Kondo effect which lifts the degeneracy at temperatures well below the new SU(2) Kondo energy scale [see the lower panel in Fig. 10 for a comparison between the entropy evolution for the asymmetric coupled triple dot case and the universal SU(2) Kondo model]. This happens because the dot 1 becomes effectively decoupled from the other two; the two remaining active dots are then effectively described by the standard twofold-degenerate single-impurity Anderson model.

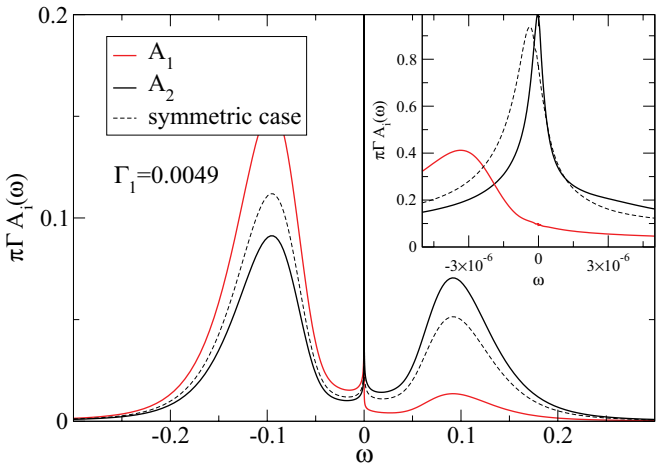

FIG. 11. (Color online) Spectral functions in the case of nonequal hybridizations Γ_i. The dashed line corresponds to the fully symmetric case with $\Gamma \equiv \Gamma_i = 0.005$.

If, however, Γ_1 is increased above $\Gamma_2 = \Gamma_3$ rather than decreased, the system crosses over from the SU(3) local-moment fp to the frozen-impurity fp without any Kondo screening (results not shown). This happens because the strong charge fluctuations on dot 1 for $\Gamma_1 > \Gamma_2 = \Gamma_3$ make it impossible for the other two dots to realize a coherent SU(2) Kondo singlet state. The same scenario occurs when all three Γ_i are different.

As already mentioned, the asymmetry of the lead-dot couplings in the SU(3) Kondo effect is analogous to the SU(2) Kondo physics in the presence of ferromagnetic contacts. In the latter case, the Kondo resonance is split due to the appearance of an induced exchange field because of the polarized contacts. The same physical behavior is obtained for the SU(3) Kondo case. Figure 11 shows this result. We plot the spectral densities for dot 1 and dot 2, denoted as $A_1(\omega)$ and $A_2(\omega)$. We consider the case of symmetric couplings ($\Gamma = \Gamma_1 = \Gamma_2 = \Gamma_3$) in which $A_1(\omega) = A_2(\omega)$ and the case of the asymmetric lead-dot coupling configuration in which $\Gamma_2 = \Gamma_3 = 0.005$ and $\Gamma_1 = 0.003$. In the latter case, the two spectral functions exhibit SU(3) Kondo-peak splitting, which can be seen more clearly in the closeup shown as an inset in Fig. 11. It is noteworthy that the Kondo spectral peaks for $A_2 = A_3$ reach a high value (approaching, in fact, the unitary limit), while that for A_1 is strongly suppressed. This is related to the fact that dots 2 and 3 are SU(2) Kondo screened, thus their zero-bias conductance remains nearly unitary, while dot 1 becomes decoupled and is only weakly conducting.

B. Unequal on-site dot energies

The SU(3) Kondo state can also be destroyed by having nonequal dot level energies. This case is illustrated in Fig. 12, where it is shown how the SU(3) symmetry is broken by changing the on-site energy ϵ_1 away from the common value ϵ, i.e., $\epsilon_1 = \epsilon + \delta\epsilon_1$, with $\delta\epsilon_1$ being the detuning. The resulting state depends on the direction of the detuning. For positive detuning $\delta\epsilon_1 > 0$, shown in the upper panel in Fig. 12, the SU(3) Kondo effect is quenched on the energy scale of the detuning. This happens because for this type of detuning, dot

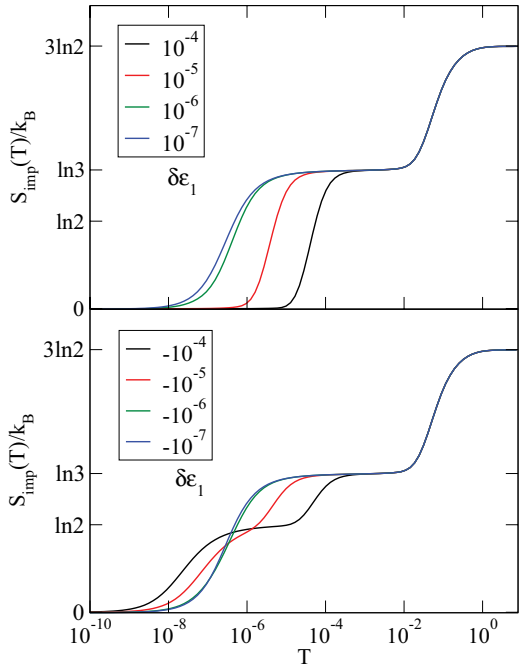

FIG. 12. (Color online) Temperature dependence of the impurity entropy for a range of the parameter $\delta\epsilon_1$ defined as $\epsilon_1 = \epsilon + \delta\epsilon_1$, while $\epsilon_2 = \epsilon_3 = \epsilon$ with $\epsilon = -0.3$. The rest of the parameters correspond to a symmetric triple quantum dot configuration with $V = 0.2$ and $\Gamma = 0.005$.

1 strongly depopulates on the temperature scale of $\delta\epsilon_1$ from $\langle n_1 \rangle \approx 2/3$ toward some small value (essentially zero for large $\delta\epsilon_1$), while the occupancy of dots 2 and 3 increases toward 1. The configuration thus corresponds to a nondegenerate quenched state, hence the direct transition to zero impurity entropy. Physically, this behavior can be explained by the fact that the threefold-degenerate local-moment state with two electrons at high temperatures consists of three states with energy $\epsilon_i + \epsilon_j + V$. In the symmetric high-temperature state, the three states are equally populated, thus $\langle n_i \rangle \approx 2/3$. If, however, $\epsilon_1 > \epsilon_2 = \epsilon_3$, the *two* many-body states where dot 1 is occupied will be depopulated.

For negative detuning $\delta\epsilon_1 < 0$, shown in the lower panel in Fig. 12, the system evolves from the threefold-degenerate local moment fp with $S_{\rm imp} = \ln 3$ to a twofold-degenerate local moment fp in which $S_{\rm imp} = \ln 2$. In this case, the SU(2) local moment emerges from two states that originally formed the SU(3) triplet local moment. This can be explained again using arguments similar to those given above: the higher-energy many-body state where dot 1 is *not* occupied is quenched, while the two remaining lower-energy states play the role of a SU(2) doublet. The local occupancies in this case are thus $\langle n_1 \rangle \approx 1$ and $\langle n_2 \rangle = \langle n_3 \rangle \approx 1/2$.

C. Finite interdot tunneling: $t \neq 0$

We have also investigated the fact that the threefold symmetry can also be broken by a finite interdot tunneling. The behavior, yet again, depends on the sign of the symmetry-breaking parameter (here t): the ground state may either be a single state (not Kondo screened) or a twofold-degenerate pair

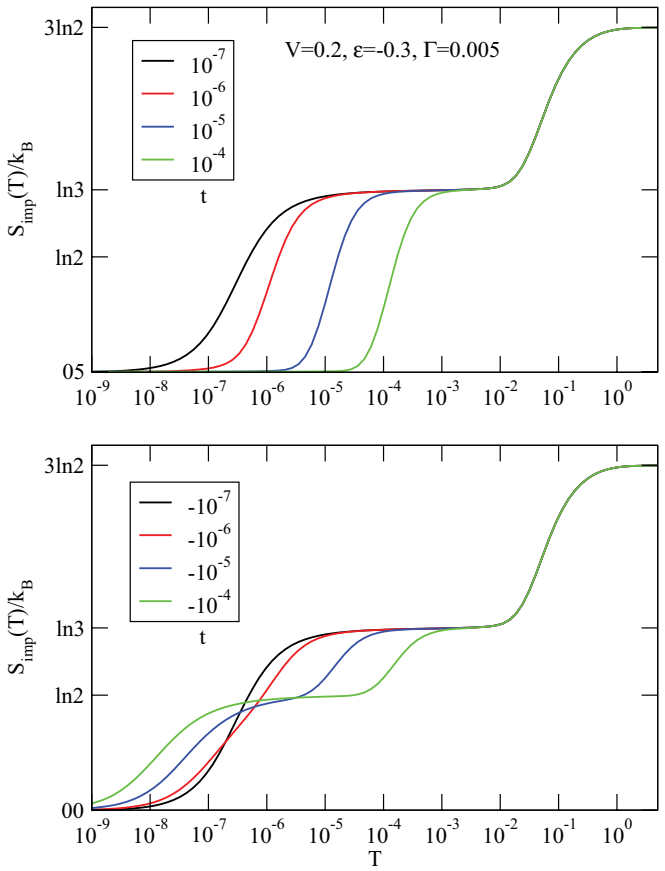

FIG. 13. (Color online) Temperature dependence of the triple quantum dot entropy for different values of interdot tunneling.

which is Kondo screened. The positive t case is considered in the upper panel of Fig. 13. Here the entropy evolves from ln 3 to zero on the temperature scale of t signaling the destruction of the SU(3) Kondo singlet. For negative t, the lower panel in the figure shows that the impurity entropy evolves from ln 3 to ln 2 on the temperature scale of $|t|$ and the latter corresponds to local moment fp of the pair of states and it constitutes a SU(2) local moment which undergoes the SU(2) Kondo screening at much lower temperatures.

This behavior is a simple consequence of the spectrum of a three-site tight-binding chain with periodic boundary conditions:

$$\epsilon_n = -2t\cos k_n, \tag{18}$$

with $k_n = 2\pi/3n$ and $n = 0, \pm 1$, i.e.,

$$\epsilon_0 = -2t, \quad \epsilon_{\pm 1} = t. \tag{19}$$

Thus for positive t the ground state is a single state, while for negative t it is a pair of states. Performing a perturbative calculation with the three many-body states forming the high-temperature local-moment multiplet, one can in an analogous way explain the behavior observed in Fig. 13.

If the tunneling parameters are all different (which would be the generic situation), the behavior will depend on the signs of the hopping parameters and their pairwise differences.

D. Restoration of the SU(3) Kondo physics

Symmetry can also be broken by having different interdot charge repulsion parameters V_{ij}. In experiments, the capacitive couplings V_{ij} are the most difficult to control, followed by the interdot hopping parameters t_{ij} and hybridizations Γ_i, while the on-site energies ϵ_i are typically the easiest to tune. There are eight "directions" for an SU(3) symmetry-breaking field, corresponding to the eight generators of this symmetry. A consideration of the Gell-Mann matrices suggests that two (λ_3 and λ_8) are associated with the energy levels, since they are diagonal, while the remaining six are out-of-diagonal and thus associated with the interdot tunneling. This immediately suggests that symmetry breaking by tunneling cannot be compensated electrostatically. It is thus essential, first of all, to ensure that the interdot tunneling is low enough for the observation of the SU(3) Kondo effect. In essence, the tunneling rate should be much smaller than the anticipated Kondo temperature scale (in appropriate frequency units). Any remaining asymmetry then corresponds to SU(3) "fields" in the λ_3 and λ_8 directions which arise from asymmetric ϵ_i, Γ_i, and V_{ij}. Assuming that the three on-site energies ϵ_i can be freely and independently tuned, it appears possible to compensate the asymmetries in Γ_i and V_{ij} since there are three parameters to drive the two symmetry-breaking "fields" to zero. We demonstrate this procedure in Fig. 14, where an asymmetry in the hybridization constants is compensated by tuning the on-site potentials. Thus, making use of the high degree of tunability in QD devices, any source of symmetry breaking which naturally arises from the manufacturing process can be compensated by properly adjusting the gate voltages.

VI. SPINFUL TRIPLE QUANTUM DOT

The spinless model that has been the focus of this work arises as an effective model from some spinful model in the

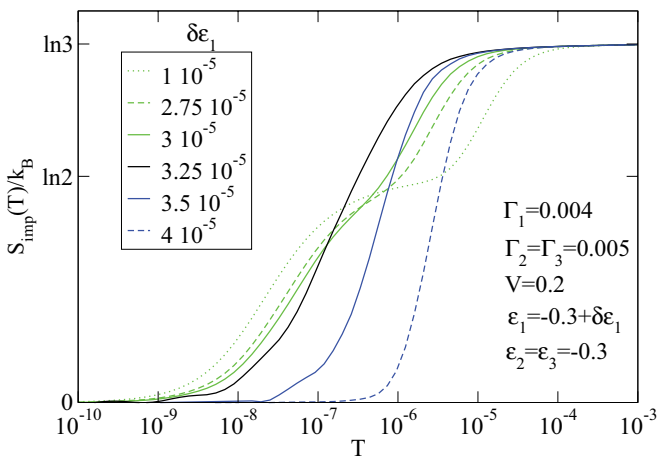

FIG. 14. (Color online) Restoration of the SU(3) Kondo effect in an asymmetrically lead-dot coupled triple quantum dot ($\Gamma_1 = 0.004$ and $\Gamma_2 = \Gamma_3 = 0.005$) by tuning the on-site dot potential $\epsilon_1 = \epsilon + \delta\epsilon_1$, with $V = 0.2$ and $\epsilon = -0.3$. The SU(3) symmetry is effectively restored for $\delta\epsilon_1 = 3.25 \times 10^{-5}$, which is indicated by the impurity curve having the universal SU(3) shape. The curves for parameters near the restoration point show some wiggles; these are numerical artifacts due to the z-averaging in NRG.

limit of a strong external magnetic field. For experimentalists, it would be interesting to know how the properties of the spinful model evolve as the magnetic field is gradually increased, since the field is never infinitely large. A systematic study of this kind is well beyond the scope of this work. However, as a first step in this direction, in this section we briefly discuss the simplest spinful "parent" model, i.e., the version of our model with spin degrees of freedom and, thus, additional on-site electron-electron repulsion terms U. The Hamiltonian takes the form of three copies of the single-impurity Anderson model and a coupling term with all interdot terms:

$$H = \sum_{i=1}^{3} H_i + H_{\text{int}}, \tag{20}$$

with

$$H_i = \sum_{k,\sigma} \epsilon_k c^\dagger_{k,\sigma,i} c_{k,\sigma,i} + \epsilon_i n_i + U_i n_{\uparrow,i} n_{\downarrow,i} + v_i \sum_{k,\sigma} (c^\dagger_{k,\sigma,i} d_{\sigma,i} + \text{H.c.}) \tag{21}$$

and

$$H_{\text{int}} = \sum_{\langle i,j \rangle} \left[V_{ij} n_i n_j + t_{ij} \sum_{\sigma} (d^\dagger_{\sigma,i} d_{\sigma,j} + \text{H.c.}) \right]. \tag{22}$$

Most terms have the same meaning as in the spinless model, Eq. (1), but now $n_{\sigma,i} = d^\dagger_{\sigma,i} d_{\sigma,i}$ and $n_i = n_{\uparrow,i} + n_{\downarrow,i}$.

Here we will only consider some features of this model. We restrict our attention to a model with no interdot tunneling, $t_{ij} \equiv 0$, and full orbital symmetry, i.e., $\epsilon_i \equiv \epsilon$, $U_i \equiv U$, $V_{ij} \equiv V$, and $v_i \equiv v$ (or, equivalently, $\Gamma_i \equiv \Gamma$). This model is too complex to be studied in detail using our implementation of the NRG (see Refs. 79 and 58 for some recent calculations for three-orbital problems using an NRG code which can explicitly take into account high-rank non-Abelian symmetries). For this reason, we resort to a different numerical approach, the Gunnarson-Schönhammer variational method. Following Refs. 77 and 78, we form a variational ansatz for the ground-state wave function $|0\rangle$ of the Hamiltonian (20),

$$|0\rangle = \sum_{n_1 n_2 n_3} \lambda_{n_1 n_2 n_3} P_{n_1 n_2 n_3} |\tilde{0}\rangle + \sum_{k,i,n_1 n_2 n_3} \lambda^{d\to k,i}_{n_1 n_2 n_3} P_{n_1 n_2 n_3} \sum_{\sigma} c^\dagger_{k,\sigma,i} d_{\sigma,i} |\tilde{0}\rangle + \sum_{k,i,n_1 n_2 n_3} \lambda^{k\to d,i}_{n_1 n_2 n_3} P_{n_1 n_2 n_3} \sum_{\sigma} d^\dagger_{\sigma,i} c_{k,\sigma,i} |\tilde{0}\rangle. \tag{23}$$

Here $|\tilde{0}\rangle$ is the ground-state wave function of the noninteracting part ($U = V = 0$) of the Hamiltonian (20) with renormalized dot energy levels $\tilde{\epsilon}$ and lead-dot couplings $\tilde{v}$,

$$\tilde{H}(\tilde{\epsilon}, \tilde{v}) = \sum_{k,\sigma,i} \epsilon_k c^\dagger_{k,\sigma,i} c_{k\sigma,i} + \sum_i \tilde{\epsilon} n_i + \sum_{k,\sigma,i} (\tilde{v} d^\dagger_{\sigma,i} c_{k\sigma,i} + \text{H.c.}). \tag{24}$$

Projectors $P_{n_1 n_2 n_3}$ project this state to subspaces with $n_i = 0,1,2$ electrons in the ith dot. Variational terms in the second and the third row of Eq. (23) provide states containing an electron above the Fermi energy and a hole below the Fermi energy in one of the leads, respectively. An approximation to the true Hamiltonian (20) ground-state energy $E_0(\tilde{\epsilon}, \tilde{v})$ and the corresponding ground-state wave-function coefficients λ are calculated by solving the Schrödinger equation within the Hilbert space of the ansatz. The ground-state energy is then further minimized with respect to $\tilde{\epsilon} \to \tilde{\epsilon}_0$ and $\tilde{v} \to \tilde{v}_0$, providing us with the noninteracting part of the Fermi liquid quasiparticle Hamiltonian $\tilde{H}(\tilde{\epsilon}_0, \tilde{v}_0)$ of our problem, which we use to calculate the zero-temperature conductance. The occupancy of the dots and its fluctuations are calculated from the ground-state wave function $|0\rangle$.

To study the interplay of the intersite and on-site charge repulsion terms U and V, we first fix U and increase V. For $V = 0$, the system consists simply of three copies of the single-impurity Anderson model, the properties of which are well known.[62,63] In the interval $-U + \Gamma \lesssim \epsilon \lesssim -\Gamma$, we expect the emergence of the SU(2) Kondo effect in each of the three channels independently, thus a plateau of unitary conductance through each dot (note that the unitary limit is now $2e^2/h$ due to the spin factor). For nonzero but moderate $V < U$, we expect the occurrence of collective Kondo screening which affects all three quantum dots. In this case, in addition to the spin degree of freedom on each dot, there is an orbital degree of freedom, as in the spinless case that has been discussed in the previous sections. The two degrees of freedom may become intertwined as in the SU(4) Kondo effect in carbon nanotubes,

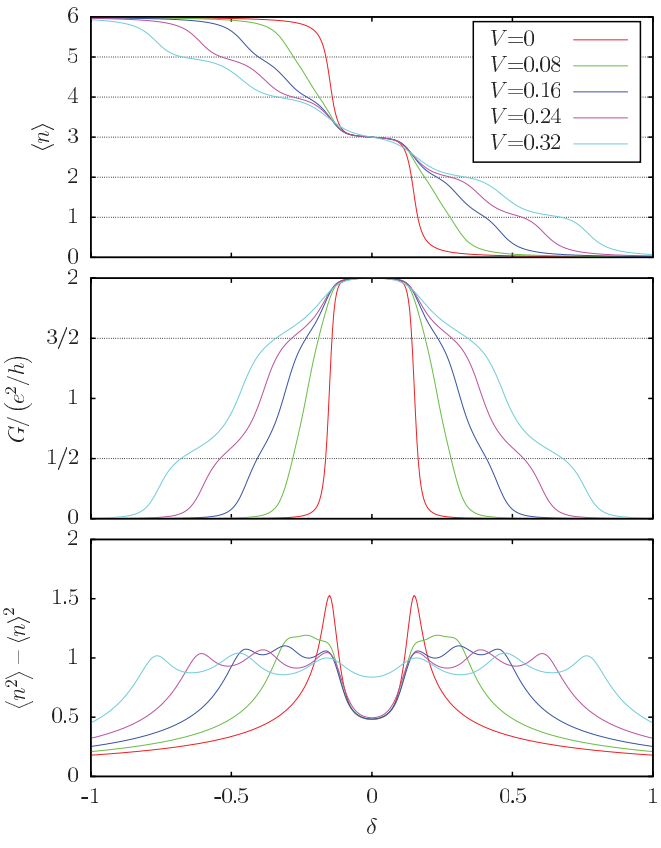

FIG. 15. (Color online) Occupancy n, differential conductance G, and charge fluctuations $\delta n^2 = \langle n^2 \rangle - \langle n \rangle^2$ as a function of the on-site energy $\epsilon = -U/2 - 2V + \delta$ for on-site repulsion $U = 0.32$ and for a range of interdot repulsions V. $\Gamma = 0.01$.

where the spin and isospin degrees of freedom are combined. Here, however, the symmetry is $SU(2)_{spin} \times SU(3)_{orbital}$ and richer behavior is expected. The results in Fig. 15 indicate the emergence of three different kinds of Kondo plateaus for on-site energies corresponding to the total TQD occupancy being pinned to an integer value. At the *p-h* symmetric point, we observe a Kondo plateau for all values of $V \leqslant U$; this is thus contrary to the behavior found in the spinless model where in this regime the valence fluctuates and the Kondo effect does not occur. Two additional types of Kondo effects are present, one for single-electron (single-hole) occupancy, $\langle n \rangle = 1,5$, characterized by the conductance pinned to $G = 2e^2/h \sin^2[(\pi/2)(1/3)] = 0.5(e^2/h)$, and the other for two-electron (two-hole) occupancy, $\langle n \rangle = 2,4$, characterized by $G = 2e^2/h \sin^2[(\pi/2)(2/3)] = 1.5(e^2/h)$. In the first case, the single electron has both spin and orbital degrees of freedom [both in the fundamental SU(2) and SU(3) representations], thus this corresponds to the SU(6) Kondo effect. In the second case, two electrons are combined into a more complex object, which is then Kondo-screened.

VII. CONCLUSIONS

We have discussed the formation of the SU(3) singlet Kondo state in a spinless triple quantum dot system. We have performed a thermodynamics analysis with the help of the susceptibility (χ_{imp}) and the impurity entropy (S_{imp}). For a highly symmetric triple quantum dot, we find, when the dot system charge is either $n = 2$ or 1, that the system evolves from the free-orbital regime at high temperatures with $T\chi_{imp} = 1$ and $S_{imp} = \ln 8$ to the threefold-degenerate local moment fixed point with $T\chi_{imp} = 4/3$ and $S_{imp} = \ln 3$ toward a nondegenerate strong-coupling fixed point where the SU(3) spin is totally screened. This crossover occurs on an exponentially low-temperature scale, $\ln T_K \propto -1/\Gamma$. In contrast, for the electron-hole symmetric point, the system evolves from the free-orbital regime to a valence-fluctuating fixed point where the entropy $S_{imp} = \ln 6$, and then to zero on the scale of Γ. Additionally, we have investigated possible perturbations that affect the formation of the SU(3) singlet Kondo state in real setups. Among these perturbations, we have studied how nonsymmetric lead-dot couplings, on-site potential energies, and finite interdot tunneling rates break the SU(3) Kondo physics. We have described the procedure to restore the SU(3) Kondo physics in real systems by tuning the on-site dot energies. Finally, we described the more complex behavior of the spinful case in which the Kondo effect occurs for all integer occupancies of the triple quantum dot, including at the particle-hole symmetric point. It would be very interesting to extend this study to the case with an external magnetic field and study the evolution of the properties from the spinful to the spinless triple impurity model.

ACKNOWLEDGMENTS

R.L. was supported by Spanish MICINN (Grants No. FIS2008-00781 and No. FIS2011-23526). T.R. and R.Ž. acknowledge the support of the Slovenian Research Agency (ARRS) under Program No. P1-0044. This work was supported by the EUFP7 project SE2ND [271554] and by a Polish grant for science.

[1] A. C. Hewson, Phys. Rev. Lett. **70**, 4007 (1993).
[2] T. K. Ng and P. A. Lee, Phys. Rev. Lett. **61**, 1768 (1988).
[3] L. I. Glazman and M. E. Raikh, JETP Lett. **47**, 452 (1988).
[4] Y. Meir, N. S. Wingreen, and P. A. Lee, Phys. Rev. Lett. **70**, 2601 (1993).
[5] D. Goldhaber-Gordon, H. Shtrikman, D. Mahalu, D. Abusch-Magder, U. Meirav, and M. A. Kastner, Nature (London) **391**, 156 (1998).
[6] S. M. Cronenwett, T. H. Oosterkamp, and L. P. Kouwenhoven, Science **281**, 540 (1998).
[7] W. G. van der Wiel, S. D. Franceschi, T. Fujisawa, J. M. Elzerman, S. Tarucha, and L. P. Kouwenhoven, Science **289**, 2105 (2000).
[8] L. P. Kouwenhoven, T. H. Oosterkamp, M. W. S. Danoesastro, M. Eto, D. G. Austing, T. Honda, and S. Tarucha, Science **278**, 1788 (1997).
[9] J. Schmid, J. Weis, K. Eberl, and K. v. Klitzing, Physica B **256–258**, 182 (1998).
[10] D. C. Ralph and R. A. Buhrman, Phys. Rev. Lett. **72**, 3401 (1994).
[11] A. Kogan, S. Amasha, and M. A. Kastner, Science **304**, 1293 (2004).
[12] S. De Franceschi, R. Hanson, W. G. van der Wiel, J. M. Elzerman, J. J. Wijpkema, T. Fujisawa, S. Tarucha, and L. P. Kouwenhoven, Phys. Rev. Lett. **89**, 156801 (2002).
[13] D. Sánchez and R. López, Phys. Rev. B **71**, 035315 (2005).
[14] R. Aguado and D. C. Langreth, Phys. Rev. Lett. **85**, 1946 (2000).
[15] A. Fuhrer, T. Ihn, K. Ensslin, W. Wegscheider, and M. Bichler, Phys. Rev. Lett. **93**, 176803 (2003).
[16] W. Hofstetter and G. Zaránd, Phys. Rev. B **69**, 235301 (2004).
[17] A. Kogan, G. Granger, M. A. Kastner, D. Goldhaber-Gordon, and H. Shtrikman, Phys. Rev. B **67**, 113309 (2003).
[18] M. Pustilnik, L. I. Glazman, and W. Hofstetter, Phys. Rev. B **68**, 161303(R) (2003).
[19] M. Pustilnik and L. I. Glazman, Phys. Rev. B **64**, 045328 (2001).
[20] S. Sasaki, S. de Franceschi, J. M. Elzerman, W. G. van der Wiel, M. Eto, S. Tarucha, and L. P. Kouwenhoven, Nature (London) **405**, 764 (2000).
[21] S. Amaha, T. Hatano, T. Kubo, Y. Tokura, D. G. Austing, and S. Tarucha, Physica E **40**, 1322 (2008).
[22] M. C. Rogge and R. J. Haug, Phys. Rev. B **77**, 193306 (2008).
[23] A. K. Mitchell, T. F. Jarrold, and D. E. Logan, Phys. Rev. B **79**, 085124 (2009).
[24] L. Gaudreau, S. A. Studenikin, A. S. Sachrajda, P. Zawadzki, A. Kam, J. Lapointe, M. Korkusinski, and P. Hawrylak, Phys. Rev. Lett. **97**, 036807 (2006).
[25] G. Granger, L. Gaudreau, A. Kam, M. Pioro-Ladrière, S. A. Studenikin, Z. R. Wasilewski, P. Zawadzki, and A. S. Sachrajda, Phys. Rev. B **82**, 075304 (2010).
[26] R. Raussendorf and H. J. Briegel, Phys. Rev. Lett. **86**, 5188 (2001).

[27]D. S. Saraga and D. Loss, Phys. Rev. Lett. **90**, 166803 (2003).
[28]J. Nygard, D. H. Cobden, and P. E. Lindelof, Nature (London) **408**, 342 (2000).
[29]T. W. Odom, J.-L. Huang, C. L. Cheung, and C. M. Lieber, Science **290**, 1549 (2000).
[30]P. Jarillo-Herrero, J. Kong, H. S. J. van der Zant, C. Dekker, and L. Kouwenhoven, Nature (London) **434**, 484 (2005).
[31]J. S. Lim, M.-S. Choi, M. Y. Choi, R. López, and R. Aguado, Phys. Rev. B **74**, 205119 (2006).
[32]A. Makarovski, J. Liu, and G. Finkelstein, Phys. Rev. Lett. **99**, 066801 (2007).
[33]D. Jacob and G. Kotliar, Phys. Rev. B **82**, 085423 (2010).
[34]C. A. Büsser, E. Vernek, P. Orellana, G. A. Lara, E. H. Kim, A. E. Feiguin, E. V. Anda, and G. B. Martins, Phys. Rev. B **83**, 125404 (2011).
[35]P. S. Cornaglia, G. Usaj, and C. A. Balseiro, Phys. Rev. Lett. **102**, 046801 (2009).
[36]F. B. Anders, D. E. Logan, M. R. Galpin, and G. Finkelstein, Phys. Rev. Lett. **100**, 086809 (2008).
[37]J. S. Lim, R. López, G. L. Giorgi, and D. Sánchez, Phys. Rev. B **83**, 155325 (2011).
[38]O. Klochan, A. P. Micolich, A. R. Hamilton, K. Trunov, D. Reuter, and A. D. Wieck, Phys. Rev. Lett. **107**, 076805 (2011).
[39]L. Borda, G. Zaránd, W. Hofstetter, B. I. Halperin, and J. von Delft, Phys. Rev. Lett. **90**, 026602 (2003).
[40]R. López, D. Sánchez, M. Lee, M.-S. Choi, P. Simon, and K. Le Hur, Phys. Rev. B **71**, 115312 (2005).
[41]S. Sasaki, S. Amaha, N. Asakawa, M. Eto, and S. Tarucha, Phys. Rev. Lett. **93**, 017205 (2004).
[42]W. Liang, M. Bockrath, and H. Park, Phys. Rev. Lett. **88**, 126801 (2002).
[43]D. H. Cobden and J. Nygård, Phys. Rev. Lett. **89**, 046803 (2002).
[44]M.-S. Choi, R. López, and R. Aguado, Phys. Rev. Lett. **95**, 067204 (2005).
[45]S. Amasha, J. Keller, I. Rau, A. Carmi, J. Katine, H. Shtrikman, Y. Oreg, and D. Goldhaber-Gordon, arXiv:1207.0526.
[46]N. Andrei, K. Furuya, and J. H. Lowenstein, Rev. Mod. Phys. **55**, 331 (1983).
[47]N. Grewe, Eur. Phys. J. B **53**, 271 (1983).
[48]Y. Kuramoto, Eur. Phys. J. B **53**, 37 (1983).
[49]N. E. Bickers, Rev. Mod. Phys. **59**, 845 (1987).
[50]D. M. Newns and N. Read, Adv. Phys. **36**, 799 (1987).
[51]J. Otsuki and Y. Kuramoto, J. Phys. Soc. Jpn. **75**, 064707 (2006).
[52]J. Otsuki, H. Kusunose, P. Werner, and Y. Kuramoto, J. Phys. Soc. Jpn. **76**, 114707 (2007).
[53]A. Carmi, Y. Oreg, and M. Berkooz, Phys. Rev. Lett. **106**, 106401 (2011).
[54]C. Mora, Phys. Rev. B **80**, 125304 (2009).
[55]C. Mora, P. Vitushinsky, X. Leyronas, A. A. Clerk, and K. Le Hur, Phys. Rev. B **80**, 155322 (2009).
[56]R. Sakano, A. Oguri, T. Kato, and S. Tarucha, Phys. Rev. B **83**, 241301 (2011).
[57]S. F. Duki, Phys. Rev. B **83**, 134423 (2011).
[58]Cătălin Paşcu Moca, Arne Alex, Jan von Delft, and Gergely Zaránd, Phys. Rev. B **86**, 195128 (2012).
[59]P. Zinn-Justin and N. Andrei, Nucl. Phys. B **528**, 648 (1998).
[60]O. Parcollet, A. Georges, G. Kotliar, and A. Sengupta, Phys. Rev. B **58**, 3794 (1998).
[61]B. Coqblin and J. R. Schrieffer, Phys. Rev. **185**, 847 (1969).
[62]H. R. Krishna-murthy, J. W. Wilkins, and K. G. Wilson, Phys. Rev. B **21**, 1003 (1980).
[63]H. R. Krishna-murthy, J. W. Wilkins, and K. G. Wilson, Phys. Rev. B **21**, 1044 (1980).
[64]Y. Meir and N. S. Wingreen, Phys. Rev. Lett. **68**, 2512 (1992).
[65]K. G. Wilson, Rev. Mod. Phys. **47**, 773 (1975).
[66]R. Bulla, T. Costi, and T. Pruschke, Rev. Mod. Phys. **80**, 395 (2008).
[67]M. Yoshida, M. A. Whitaker, and L. N. Oliveira, Phys. Rev. B **41**, 9403 (1990).
[68]W. C. Oliveira and L. N. Oliveira, Phys. Rev. B **49**, 11986 (1994).
[69]J. B. Silva, W. L. C. Lima, W. C. Oliveira, J. L. N. Mello, L. N. Oliveira, and J. W. Wilkins, Phys. Rev. Lett. **76**, 275 (1996).
[70]C. A. Paula, M. F. Silva, and L. N. Oliveira, Phys. Rev. B **59**, 85 (1999).
[71]V. L. Campo and L. N. Oliveira, Phys. Rev. B **72**, 104432 (2005).
[72]R. Žitko and T. Pruschke, Phys. Rev. B **79**, 085106 (2009).
[73]R. Peters, T. Pruschke, and F. B. Anders, Phys. Rev. B **74**, 245114 (2006).
[74]A. Weichselbaum and J. von Delft, Phys. Rev. Lett. **99**, 076402 (2007).
[75]D. Goldhaber-Gordon, J. Göres, M. A. Kastner, H. Shtrikman, D. Mahalu, and U. Meirav, Phys. Rev. Lett. **81**, 5225 (1998).
[76]J. J. Parks, A. R. Champagne, T. A. Costi, W. W. Shum, A. N. Pasupathy, E. Neuscamman, S. Flores-Torres, P. S. Cornaglia, A. A. Aligia, C. A. Balseiro *et al.*, Science **328**, 1370 (2010).
[77]K. Schönhammer, Phys. Rev. B **13**, 4336 (1976).
[78]O. Gunnarsson and K. Schönhammer, Phys. Rev. B **31**, 4815 (1985).
[79]Andreas Weichselbaum, Ann. Phys. **327**, 2972 (2012).